Performance Analysis of a Dispersion Compensator Using Arrayed-Waveguide Gratings

Hiroyuki Tsuda, *Member, IEEE, Member, OSA*, Hirokazu Takenouchi, Akira Hirano, Takashi Kurokawa, *Member, IEEE, Member, OSA*, and Katsunari Okamoto, *Senior Member, IEEE, Member, OSA*

***Abstract*—We have developed a dispersion compensator that uses arrayed-waveguide gratings (AWGs) and a spatial filter. The compensator using AWGs with 380 waveguides in each array and the diffraction order of 53, can compensate a total second-order dispersion of 260 ps/nm with an eye-closure penalty of 1 dB for a 40-Gb/s nonreturn-to-zero (NRZ) signal. It is shown that the required spatial resolution of the spatial phase filter for compensation is 2.5–5 μm for silica AWGs of usual design. The acceptable fluctuation in the refractive index of the waveguides in the AWGs is as large as 5×10^{-5}.**

***Index Terms*—Arrayed-waveguide grating (AWG), dispersion compensation, dispersion compensator, gratings, optical communication, optical equalizers, optical pulse compression, optical waveguide components.**

I. Introduction

HIGH-CAPACITY photonic networks can be constructed by using 40-Gb/s-based dense wavelength-division multiplexing (DWDM) because of its high signal-spectrum efficiency and the larger tolerance it provides for lasing wavelength and filter specifications. However, not only the total second-order dispersion at the center wavelength but also the residual total second-order dispersion due to the GVD (group velocity dispersion) slope of the fiber should be compensated for because they are larger than the dispersion tolerance of 47.5 ps/nm of the 40-Gb/s-based WDM system [1], [2].

The GVD and GVD slope of the optical fiber can be compensated by a fiber grating (FG) [3], [4] or a dispersion compensating fiber (DCF) [5], [6]. Both devices can compensate a large amount of total dispersion. However, the FG has a group delay ripple which significantly degrades received optical waveforms and the DCF has difficulty in compensating the GVD and the GVD slope of a nonzero dispersion shifted fiber (NZDSF) simultaneously. The dispersion equalizer with cascaded Mach–Zehnder interferometers (MZIs) presented by Takiguchi *et al.* [7] is promising because of its tunability; however, its bandwidth is limited to about 400 GHz.

Manuscript received August 3, 1999; revised March 24, 2000.

H. Tsuda was with the NTT Photonics Laboratories, Kanagawa 243-0198, Japan. He is now with the Department of Electronics and Electrical Engineering, Keio University, Kanagawa 223-8522, Japan.

H. Takenouchi is with the NTT Photonics Laboratories, Kanagawa 243-0198, Japan.

A. Hirano is with the NTT Network Innovation Laboratories, Kanagawa 239-0847, Japan.

T. Kurokawa is with the Tokyo University of Agriculture and Technology, Tokyo 184-8588, Japan.

K. Okamoto is with the NTT Photonics Laboratories, Ibaragi 319-1196, Japan.

Publisher Item Identifier S 0733-8724(00)06473-2.

We have developed a dispersion compensator that uses arrayed-waveguide gratings (AWGs) and a spatial phase filter. And this compensator successfully demonstrated second- and third-order dispersion compensation. The results showed that the dispersion compensator would have a compensation range of $\pm$100 ps/nm for 12.5-ps pulses [8], [9]. This type of dispersion compensator is useful because it has a bandwidth of several terahertz, can compensate second- and third-order dispersion simultaneously, and can compensate negative and positive dispersion. It should be noted that a AWG with a different filter has already been used for various applications such as optical code division multiplexing [10]–[12] and optical phase-shift keying direct detection [13].

In this paper, we theoretically investigate the compensation performance of the proposed compensator in a 40-Gb/s nonreturn-to-zero (NRZ) system and we evaluated it from the viewpoints of eye-closure penalty and excess loss.

II. Principle of Dispersion Compensation by Using AWGs

The principle of dispersion compensation by using AWGs is schematically shown in Fig. 1. Dispersion compensation is performed by decomposing the input waveform of each wavelength channel into its frequency components in AWG#1, compensating the phase of each component of each wavelength channel by a spatial phase filter located on the frequency plane, and reforming the waveform by combining the components in AWG#2. Note that AWG#1 and AWG#2 are the same. We previously fabricated the dispersion compensator using the reflection configuration because the size of the substrate needed could be minimized [8], [9]. This dispersion compensation method is based on the time-to-space-conversion optical signal processing with diffraction gratings reported by Weiner *et al.* [14]. Recently, their group used a spectral phase equalizer to transmit a 400-fs pulse over a 10-km fiber [15], [16]. A geometrical explanation of the AWG-based time-to-space-conversion is shown in Appendix.

III. Theoretical Model of Dispersion Compensation by AWGs

The time-to-space-conversion optical signal processing is limited by the time window and the spectral window of the optical system. The time window is the width of the time converted to the space at a time, which is inversely proportional to the spectral resolution of the AWG. If part of the waveform is broadened beyond the time window, we cannot recover the

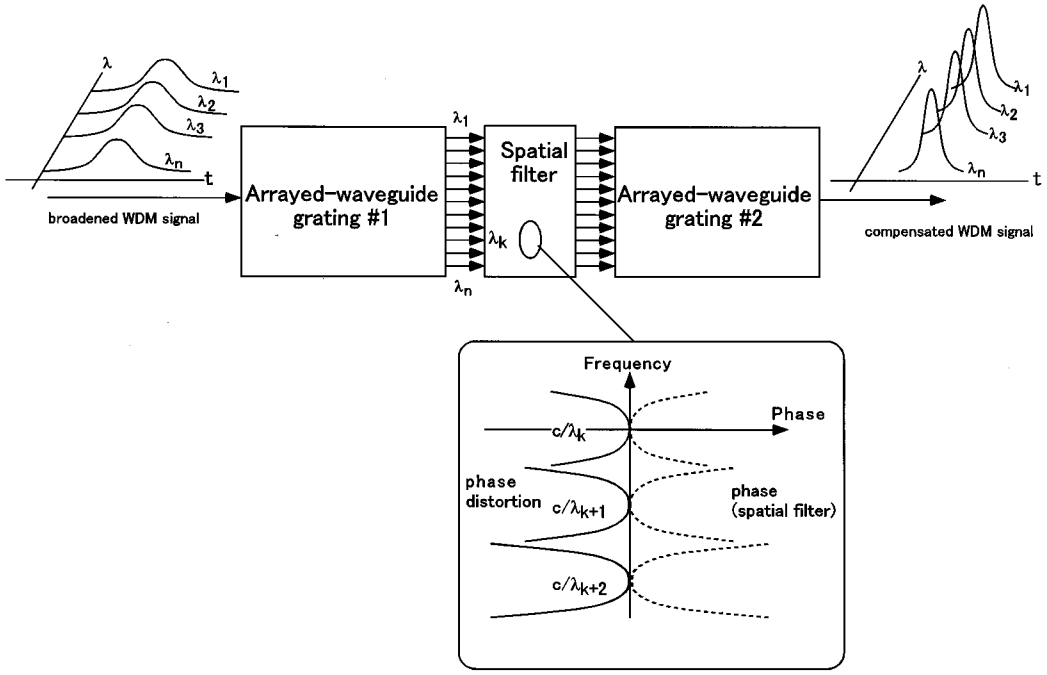

Fig. 1. Configuration of a dispersion compensator with AWGs.

original waveform. In other words, the phase distortion in a spectral plane within the resolution bandwidth has to be sufficiently small for all spectral components. The spectral window is the free spectral range (FSR or bandwidth) of the AWG, which is usually 3–5 THz and much wider than the bandwidth of the 40-Gb/s signal. Therefore, the spectral window does not affect the dispersion compensation directly; however, it should be wider than the whole bandwidth of the WDM signal.

The maximum total second-order dispersion that can be compensated for ($|D^{(2)}_{\rm tot}|$) is approximately given as [9]

$$||D^{(2)}_{\rm tot}|_{\max} < \frac{kmNT_0\nu_0}{c} \tag{1}$$

where k is a constant, m is the diffraction order, N is the number of waveguides in each array, T_0 is the full width at half maximum of the input pulse when it is completely compensated for, and ν_0 is the center frequency of optical pulses.

Most of the characteristics of the compensator are determined by m and N. Equation (1) indicates that $||D^{(2)}_{\rm tot}|$ is proportional to the resolution of the AWGs, mN/ν_0, for a given ν_0. The bandwidth is equal to the free spectral range, ν_0/m. The size of the substrate is roughly proportional to N. Fig. 2 shows the AWG design map for dispersion compensation. The bandwidth is usually adjusted to the whole bandwidth of the WDM system. When target is 16ch- or 32ch-, 200-GHz-spacing, 40-Gb/s-based WDM system, m is set to 60 or 30 to obtain the bandwidth of 3.2 or 6.4 THz. N is set to the maximum value, which is determined by the size of the substrate. The parameters of the AWG designed for 16 channel WDM system are summarized in Table I and the white circle in Fig. 2 indicates the designed values of m and N. These parameters correspond to a WDM router with a channel spacing of 30 GHz and 117

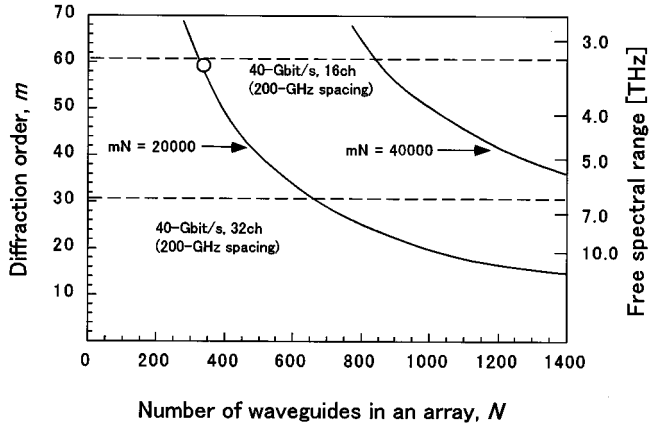

Fig. 2. AWG design map for dispersion compensation; m and FSR versus N.

channels and the AWG can be fabricated on a 50-× 50 mm substrate.

However, designing the dispersion compensator according to (1) and Fig. 2 is not sufficiently accurate because we cannot determine the value of k. It is necessary to calculate an output waveform taking the effect of finite resolution of the spatial filter and the imperfect AWG into consideration.

Fig. 3(a) shows a schematic of the first AWG, which decomposes the input signals into its spectral components. The signal input to one of the WDM channels, $\mu_{\rm in}(t)\ \exp(i\omega_c t)$, is distributed into each waveguide of the waveguide array through the slab waveguide A. It is assumed that the center angular frequency of the input signal, μ_c, is the same as that of the AWG. The light coupled to the kth waveguide is given by

$$f_{0,k}(t) = g_{1,k}u_{\rm in}(t) \tag{2}$$

TABLE I
DESIGN PARAMETERS OF AWG

Number of arrayed-waveguides	N	380	
Diffraction order	m	53	
Pitch of arrayed-waveguides	d	15	[μm]
Focal length of slab waveguide	L_f	32.222	[mm]
Effective refractive index of slab	n_s	1.45213	
Group refractive index of arrayed-waveguide	n_g	1.47332	
Effective refractive index of arrayed-waveguide	n_c	1.45013	
Center frequency	ν_c	189.268	[THz]
Free spectral range	FSR	3.51	[THz]

where $g_{1,k}$ is the distribution coefficient. Each light propagating through the waveguide in the waveguide array is skewed, and the output light from the kth waveguide into the slab waveguide B is given by

$$f_{1,k}(t) = g_{1,k} g_{2,k} u_{\text{in}} \left(t - \frac{m}{\nu_0} k \right) \tag{3}$$

where $g_{2,k}$ is the phase error due to the fluctuation of the refractive index of the waveguide. The total output waveform from the waveguide array is given by

$$f_1(x_1, t) = \sum_{n=1}^{N} g_{1,k} g_{2,k} u_{\text{in}} \left(t - \frac{m}{\nu_0} k \right) p(x_1 - kd) \tag{4}$$

where $p(x)$ is the normalized mode-field-distribution function at the edge of the arrayed-waveguide, and d is waveguide pitch. The edges of the waveguides are located on a circle, so $f_1(x_1, t)$ is Fourier transformed on the circular locus and spectrally decomposed. The waveform on the spectral locus is given by

$$f_2(x_2, t) = \alpha \int f_1(x_1, t) \exp \left(-i \frac{\omega_c n_s x_2}{c L_f} x_1 \right) dx_1 \tag{5}$$

where α is a constant, n_s is the effective refractive index of the slab waveguide, c is the velocity of light, and L_f is the focal length of the slab waveguide. The spatial phase filter, which has a transmission function of $H(x_2)$, is located on the spectral plane and modulates the phase of $f_2(x_1, t)$ and compensates the phase distortion of the input signal. The excess phase modulation due to the circular focusing locus may also be compensated by the appropriate spatial filter or lens. The waveform after the spatial filter is given by

$$f_2'(x_2, t) = f_2(x_2, t) H(x_2). \tag{6}$$

Fig. 3(b) shows the second AWG, which combines the spectral components. The waveform in front of the edge of the waveguide array (on the x_3 axis) is given by

$$f_3(x_3, t) = \alpha \int f_2(x_2) \exp \left(-i \frac{\omega_c n_s x_3}{c L_f} x_2 \right) dx_2. \tag{7}$$

The light coupled to the lth waveguide is given by

$$f_{3,l}(t) = \int f_3(x_3, t) p(x_3 - ld)\, dx_3. \tag{8}$$

It is inversely skewed as it propagates through the waveguide. The waveform at the edge of the slab waveguide D (on the x_4 axis) is given by

$$f_4(x_4, t) = \sum_{l=1}^{N} g_{3,l} f_{3,l} \left(t + \frac{m}{\nu_0} l \right) p(x_4 - ld) \tag{9}$$

where $g_{3,l}$ is the phase error due to the fluctuation of the refractive index of the waveguide. The waveform in front of the output waveguide is given by

$$f_5(x_5, t) = \alpha \int f_4(x_4, t) \cdot \exp \left(-i \frac{\omega_c n_s x_4}{c L_f} x_5 \right) dx_4 \tag{10}$$

while the output waveform is given by

$$u_{\text{out}}(t) = \int f_5(x_5, t) r(x_5)\, dx_5 \tag{11}$$

where $r(x)$ is the normalized mode-field-distribution function at the edge of the output waveguide. We can calculate the compensated waveform by using (2)–(11).

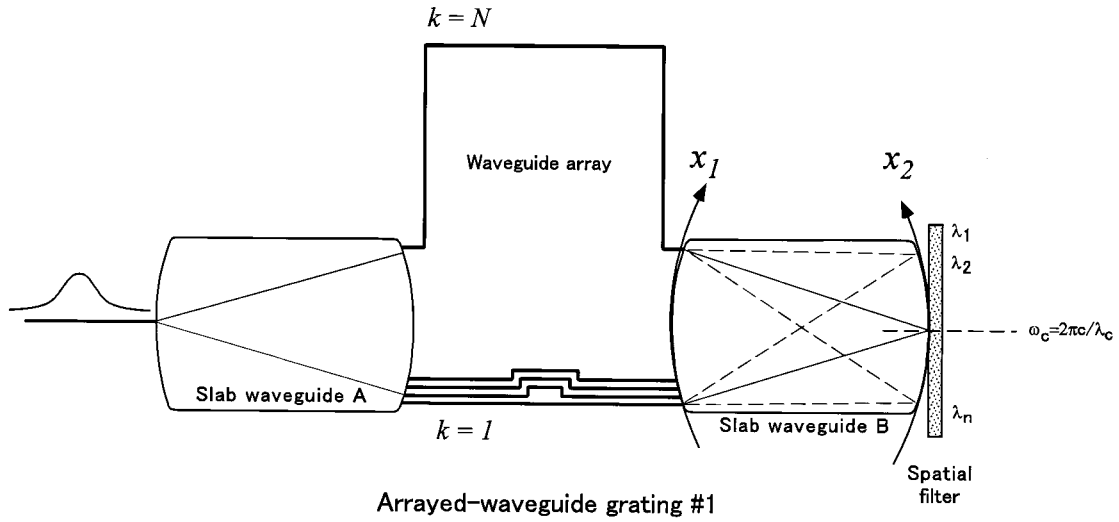

(a)

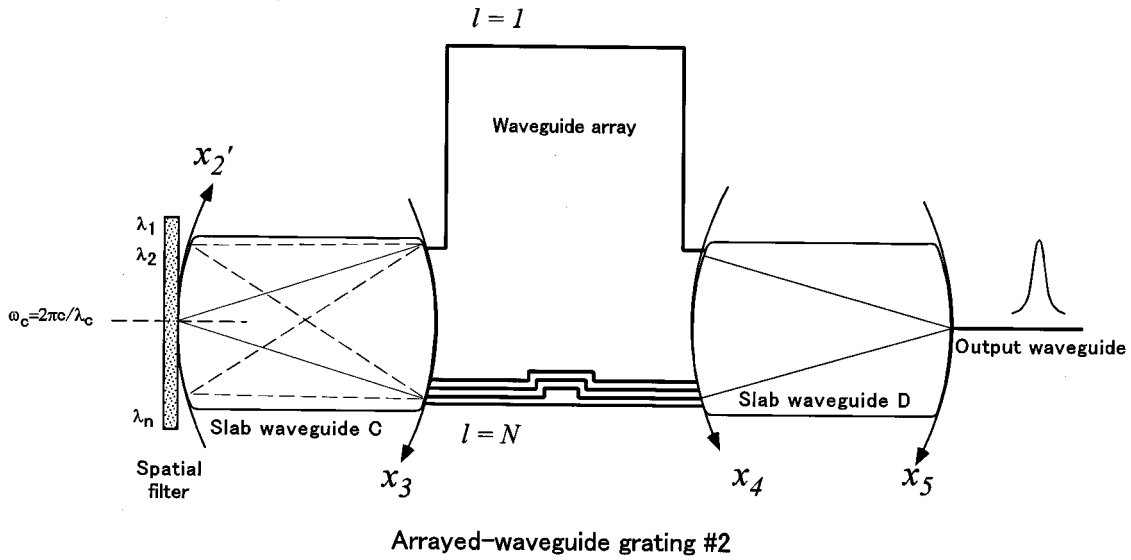

(b)

Fig. 3. (a) Schematic of the first AWG, which decomposes the input signal into its spectral components. The spatial phase filter on the spectral plane compensates the phase distortion of input signals. (b) Schematic of the second AWG, which recombines the spectral components.

IV. Dispersion Compensation Performance

The main application target of the developed dispersion compensator is the NRZ, 40-Gb/s-based WDM system because it will be cost effective if an efficient dispersion compensator is available. The dispersion-compensation performance of the compensator was estimated from the viewpoints of eye-closure penalty and excess loss for a 40-Gb/s signal. The turn-on and turn-off waveforms of the original signal were assumed to be those of super-Gaussian, respectively, with a steepness parameter of 1.6 and a width of 25 ps. It was also assumed that the original signal was not chirped. The original signal was distorted by a pure second-order dispersive medium and input to the dispersion compensator. The filter located on the spectral plane had a parabolic phase shift for correcting the phase distortion induced by the dispersive medium. The compensated signal was received by an optical receiver that had a fifth-order Bessel-Thomson filter with a 3-dB bandwidth of 28 GHz for equalizing the detected waveform.

A. Dispersion Compensation by Using Ideal AWGs and a Spatial Filter

Fig. 4(a) shows eye-closure penalty as a function of total compensated dispersion of a compensator consisting of ideal AWGs and a spatial filter. If the acceptable penalty is 1 dB, the total dispersion that can be compensated is about 260 ps/nm. It should be noted that this compensator offers the same level of negative dispersion compensation as that of positive compensation, so the dispersion compensation range is from −260 to 260 ps/nm. The value of k in (1) is calculated to be about 1.6 for the 40-Gb/s NRZ signal. The larger the total dispersion to be compensated for is, the longer the turn-on and the turn-off time of the input waveform are. The compensator can not correctly reshape the

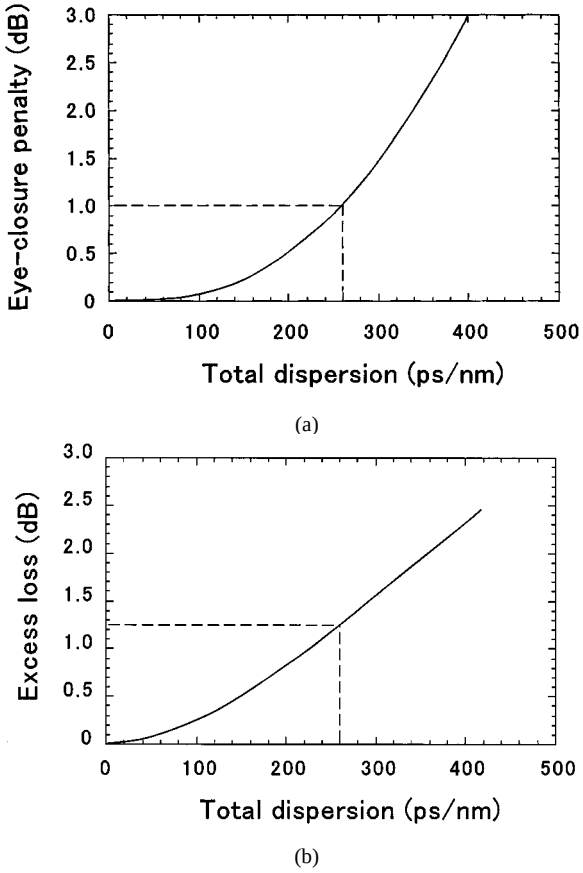

Fig. 4. (a) Eye-closure penalty as a function of total compensated dispersion when ideal AWGs and a spatial filter are used in the compensator. (b) Excess loss due to dispersion compensation as a function of total compensated dispersion when ideal AWGs and a spatial filter are used in the compensator.

part of waveform broadened over the time window. The time window is about $mN/2\nu_0 \cong 50$ ps when $m = 53$ and $N = 380$.

The excess loss due to dispersion compensation as a function of total compensated dispersion is shown in Fig. 4(b). The excess loss when compensating the total dispersion of 260 ps was less than 1.3 dB. The excess loss is attributed to the light diffracted beyond the waveguide array #2. It occurs when the residual phase distortion exists after spatial filtering. Fig. 5(a)–(d), respectively, show eye patterns of the input waveform, the back-to-back received waveform, the waveform distorted by the dispersive medium with a total dispersion of 200 ps/nm, and the compensated waveform. All the figures indicate that a clear eye-opening is obtained by using the developed dispersion compensator.

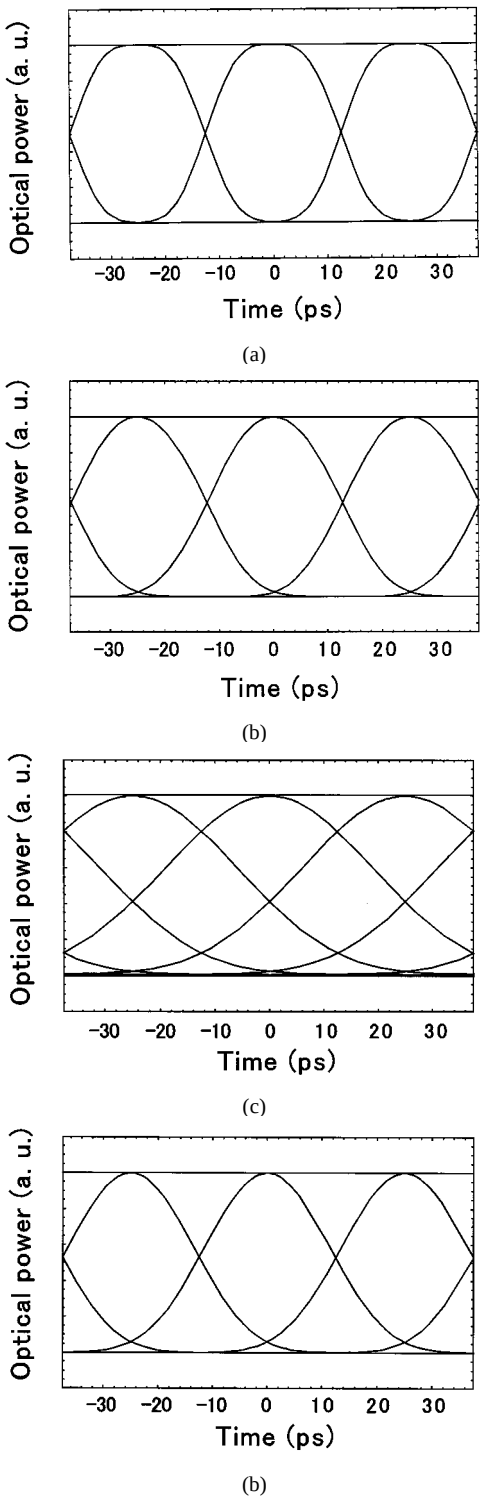

Fig. 5. (a) Eye patterns of the input waveform, (b) back-to-back received waveform, (c) waveform distorted by the dispersive medium with a total dispersion of 200 ps/nm, and (d) compensated waveform.

B. Dispersion Compensation by Using a Spatial Filter with Finite Resolution

We fabricated a spatial phase filter by electron beam lithography and the maximum spatial resolution of the filter was about 0.1 μm [8], [9]. Fabrication, however, takes a long time at the maximum resolution when drawing filters with large areas. The spatial resolution required for dispersion compensation has to be estimated. The length corresponding to the spectral resolution of the AWG, Δx, is given by

$$\Delta x = \frac{2\pi L_f c}{n_s N d\omega_c} \left(\frac{n_g}{n_c}\right) \tag{12}$$

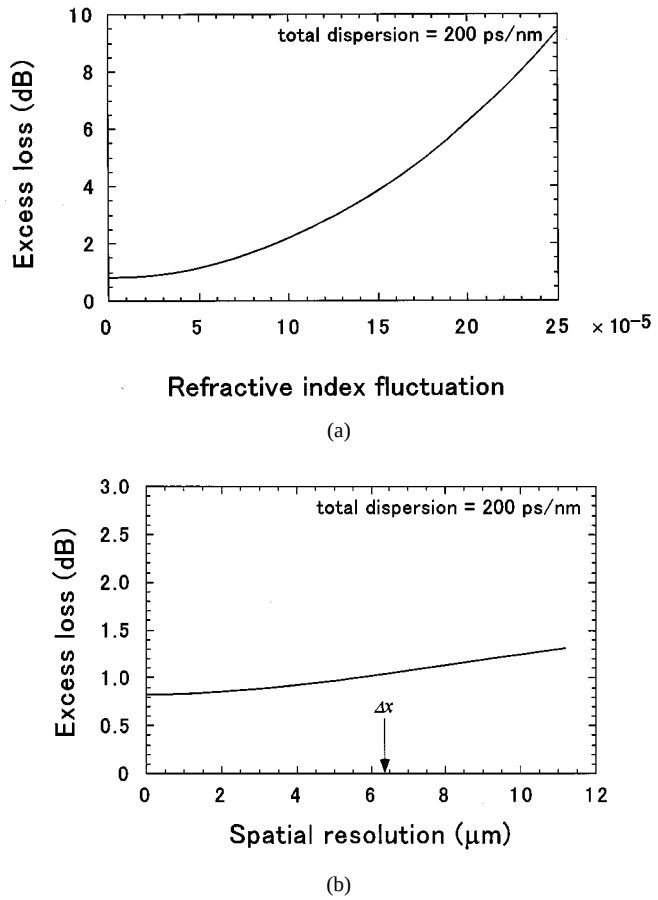

Fig. 6. (a) Eye-closure penalty as a function of the spatial resolution of the filter when compensating total dispersion of 200 ps/nm. (b) Excess loss due to dispersion compensation as a function of the spatial resolution of the filter when compensating total dispersion of 200 ps/nm.

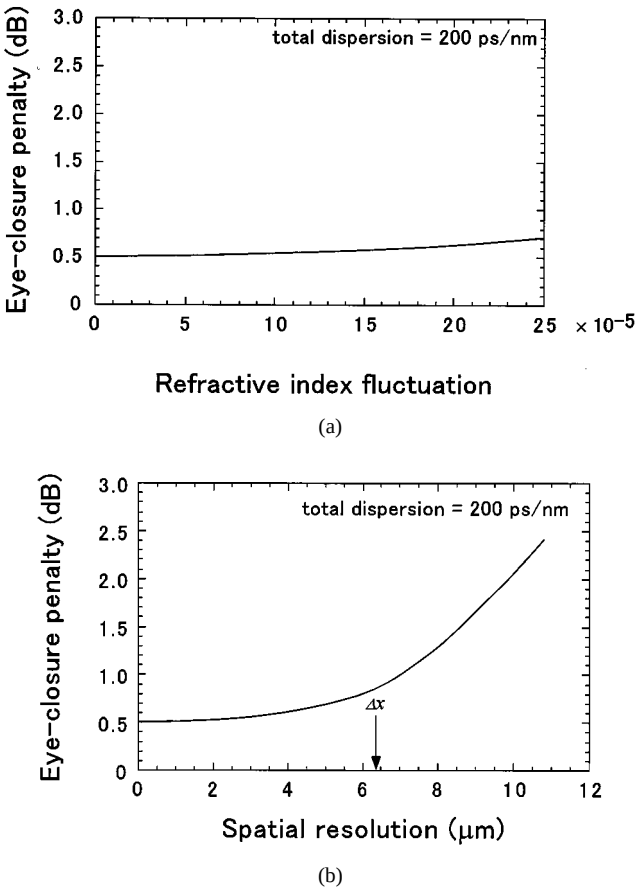

Fig. 7. (a) Eye-closure penalty as a function of the standard deviation of the refractive index fluctuation when compensating total dispersion of 200 ps/nm. (b) Excess loss due to dispersion compensation as a function of the standard deviation of the refractive index fluctuation when compensating total dispersion of 200 ps/nm.

where n_g and n_c are group refractive index and effective refractive index of the arrayed-waveguide. And Δx is usually 5–10 μm, depending on the design of the AWG. For example, when we use the parameters in Table I, Δx is 6.3 μm. Fig. 6(a) and (b) show the eye-closure penalty and the excess loss as a function of the spatial resolution of the filter when compensating total dispersion is 200 ps/nm. The excess loss is almost constant; however, the eye-closure penalty rapidly increases when the spatial resolution of the filter exceeds Δx. These results suggest that the spatial resolution of the filter has to be roughly less than a half of Δx, which is usually 2.5–5 μm.

C. Dispersion Compensation by Using Imperfect AWGs

In principle, the larger the size of the AWG is, the better the dispersion-compensating performance becomes. However, fluctuation in the refractive index significantly degrades AWG performance [11]. Fig. 7(a) and (b) show the eye-closure penalty and the excess loss as a function of the standard deviation of the refractive index fluctuation when compensating the total dispersion is 200 ps/nm. The fluctuation was assumed to be random, waveguide by waveguide, but it follows a Gaussian distribution. The excess loss increases rapidly when the refractive index fluctuation is larger than 1×10^{-4}while the eye-closure penalty increases slowly. The refractive index fluctuation was reported to be only 1.9×10^{-6} [11]. So these results indicate that the dispersion compensator using AWGs is not affected by refractive index fluctuation. This is because the effect of the fluctuation is eliminated at the joint of the output waveguide. The fluctuation causes wave-front distortion on the output of the arrayed-waveguide (x_4 axis in Fig. 3). Such distortion has a high spatial frequency due to the randomness of the fluctuation, so it does not couple into the output waveguide.

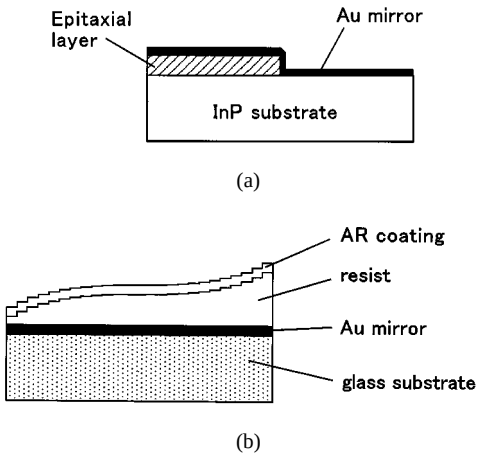

Fig. 8. (a) Structure of a spatial filter for PSK detection. (b) Structure of a spatial filter for third-order dispersion compensation.

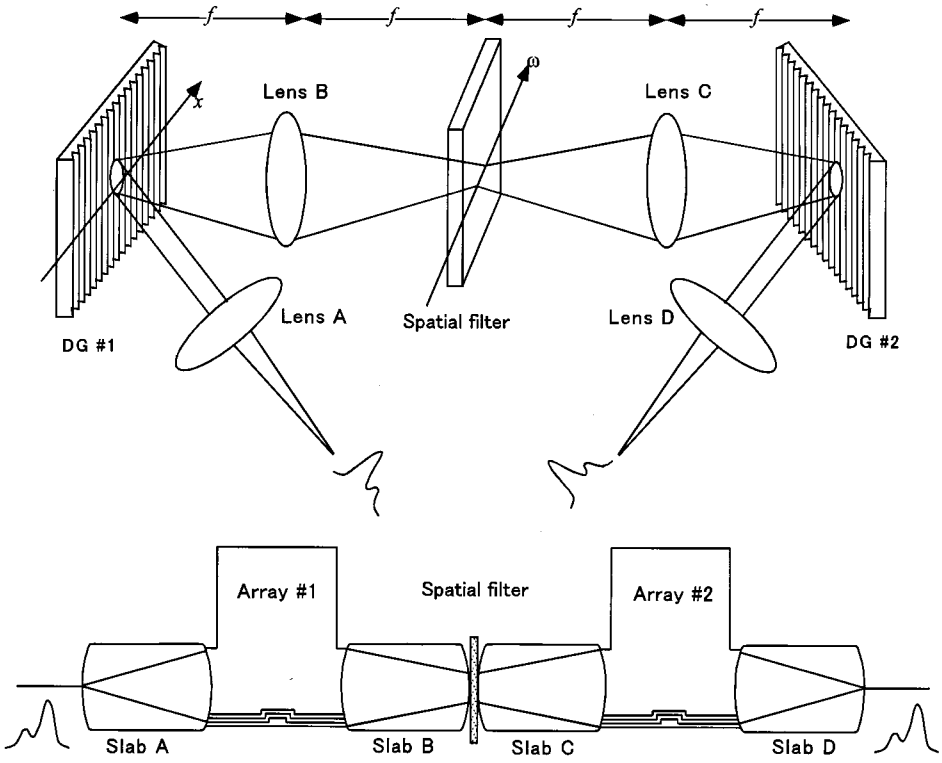

Fig. 9. Schematic configurations of the time-to-space-conversion optical signal processing using diffraction grating pairs and AWG pairs.

D. Practical Implementation

This paper focuses on the theoretical investigation of the compensation performance of developed compensator; however, losses in the compensator should be discussed: 1) the intrinsic loss of the AWG, 2) the coupling loss between two AWGs or the coupling loss between the AWG and mirror, and 3) the loss of the spatial filter. The total insertion loss including excess loss and these losses determine the signal-to-noise ratio (SNR) of the signal.

The intrinsic loss of the silica AWG configured on a 50×50 mm substrate is usually about 3 dB. The intrinsic AWG loss is mainly due to the coupling loss between a slab waveguide and a waveguide array, and the propagation loss in the waveguide is quite low. Therefore, the larger AWG would have almost the same loss. The coupling loss between the AWG and the mirror is very large without coupling lens. Recently, we have developed coupling lens, which reduces the coupling loss from about 5 to 1 dB. The lens converts the circular focal locus to a flat one to eliminate excess second-order dispersion.

We had fabricated two types of phase filter for the previously reported experiment, as shown in Fig. 8(a) and (b). The first type of filter was used for quasidifferential processing of the PSK lightwave signal for detection [13]. The loss of the filter was less than 0.2 dB. The second type of filter was used for dispersion compensation experiment and its loss was about 2 dB [8], [9]. For dispersion compensation, the second type is better because it provides high spatial resolution and fine phase steps.

The total loss is given by

$$\begin{aligned}&\text{(total loss)}\\&\quad = \text{(intrinsic AWG loss)} \times 2\\&\qquad + \text{(coupling loss between the AWG and mirror)} \times 2\\&\qquad + \text{(filter loss)} + \text{(excess loss)} + \text{(circulator loss)}\\&\quad \cong 15 \text{ dB}.\end{aligned} \tag{13}$$

The total loss is larger than that of the DCF or the FG; however, it is easily compensated by an optical amplifier with a small SNR degradation. It should be noted that the total loss does not strongly depend on the dispersion compensation capability.

V. Summary

The maximum total dispersion that can be compensated by the developed compensator is about 260 ps/nm for a 40 Gb/s-NRZ signal when the AWGs have 380 waveguides per array and the diffraction order is 53. The compensator can compensate the dispersion (including GVD and GVD slope) of one span (80–120 km) of NZ-DSF and it has the very wide spectral range of about 3.5 THz. The required spatial resolution of the phase filter located on the spectral plane is 2.5–5 μm, which is much larger than the resolution available with electron beam lithography. The excess loss or the eye-closure penalty due to the refractive index fluctuation is not significant when the fluctuation is less than 5×10^{-5}.

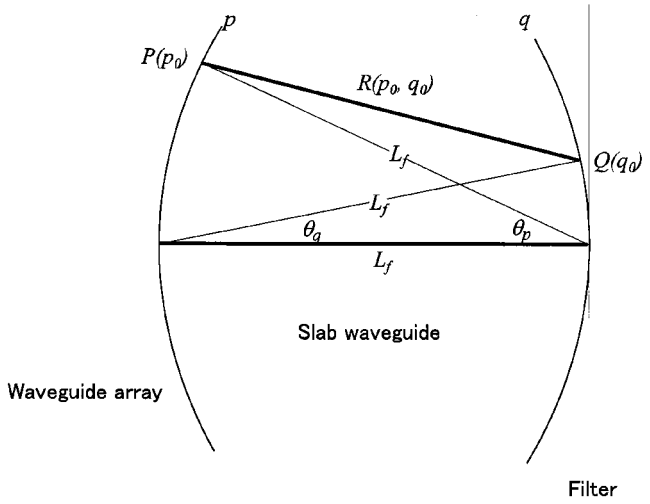

Fig. 10. Slab waveguide configuration.

These results indicate that we can scale a compensator up according to (1) and the value of k is 1.6 for the 40-Gb/s NRZ signal. The diffraction order, m, is usually determined by the whole bandwidth of the WDM system; therefore, larger N is used to obtain the higher performance compensator. The maximum size of the substrate is about 50 × 50 mm at present; however, larger substrates will be available and the compensator with higher performance will be fabricated.

APPENDIX

Time-to-space-conversion optical signal processing using AWGs is based on that of using diffraction grating pairs and a spatial filter. One can easily understand the principle of the method by comparing two types of time-to-space-conversion optical system. Fig. 9 shows both systems schematically. The first slab waveguide (Slab A) distributes an optical signal into each waveguide of the waveguide array (Array #1). The adjacent waveguides in the array have the same optical path difference and work as a diffraction grating. Slab B, and C, Array #2, and Slab D correspond to Lens B, Lens C, DG #2, and Lens D, respectively.

Fig. 10 schematically shows a slab waveguide. The edges of the waveguides are located in a circle on the locus of p and the output plane is the circular locus of q. The center of each circular locus is on the corresponding circular locus. The length of the line from the point $P(p_0)$ to the point $Q(q_0)$, $R(\theta_p, \theta_q)$ is given by

$$R(\theta_p, \theta_q) = L_f\sqrt{1 - 2\,\sin\theta_p\,\sin\theta_q + 2(1-\cos\theta_p)(1-\cos\theta_q)}. \tag{A1}$$

where L_f is the length of the slab waveguide. p_0 and q_0 are given by

$$p_0 = L_f\theta_p \tag{A2}$$

$$q_0 = L_f\theta_q, \text{ respectively.} \tag{A3}$$

Usually, θ_p and θ_q are under 0.05; therefore, (A1) is approximated to

$$R(\theta_p, \theta_q) \cong L_f(1 - \theta_p\theta_q) = L_f - \frac{p_0 q_0}{L_f}. \tag{A4}$$

Consequently, the light propagating from locus p to q has a phase term

$$\exp\left[i\,\frac{\omega}{c}\,R(p_0, q_0)\right] = \exp\left[i\,\frac{\omega_c L_f}{c}\right] \cdot \exp\left[-i\,\frac{\omega_c p_0 q_0}{c L_f}\right]. \tag{A5}$$

Equation (A5) means that the slab waveguide works as a lens and both locus p and q are Fourier planes. The detailed analysis of this geometry was reported by Dragone [18].

ACKNOWLEDGMENT

The authors are grateful to K. Kawano and M. Itoh of NTT Photonics Laboratories for their fruitful discussion on the calculation method. They also thank S. Mitachi and C. Amano of NTT Photonics Laboratories for their encouragement.

REFERENCES

[1] M. Yoneyama, Y. Miyamoto, T. Otsuji, A. Hirano, H. Kikuchi, T. Ishibashi, and H. Miyazawa, "Fully electrical 40-Gbit/s TDM system prototype and its application to 160-Gbit/s WDM transmission," in *Proc. Optical Fiber Commun. Conf. (OFC'99)*, vol. 4, Feb. 1999, pp. 128–130.

[2] K. Ennser, R. I. Laming, and M. N. Zervas, "Analysis of 40 Gb/s TDM-transmission over embedded standard fiber employing chirped fiber grating dispersion compensators," *J. Lightwave Technol.*, vol. 16, pp. 807–811, May 1998.

[3] T. Komukai and M. Nakazawa, "Fabrication of nonlinearly chirped fiber Bragg gratings for higher-order dispersion compensation," *Opt. Commun.*, vol. 154, pp. 5–8, Aug. 1998.

[4] M. Durkin, M. Ibsen, M. J. Cole, and R. I. Laming, "1m long continuously-written fiber Bragg gratings for combined second- and third-order dispersion compensation," *Electron. Lett.*, vol. 33, no. 22, pp. 1891–1893, Oct. 1997.

[5] T. Onishi, T. Kashiwada, Y. Koyano, Y. Ishiguro, M. Nishimura, and H. Kanamori, "Third-order dispersion compensating fibers for nonzero dispersion shifted fibers," *Electron. Lett.*, vol. 32, no. 25, pp. 2344–2345, Dec. 1996.

[6] C.-C. Chang and A. M. Weiner, "Fiber transmission for sub-500-fs pulses using a dispersion-compensating fiber," *IEEE J. Quantum Electron.*, vol. 33, pp. 1455–1464, Sept. 1997.

[7] K. Takiguchi, S. Kawanishi, H. Takara, A. Himeno, and K. Hattori, "Dispersion slope equalizer for dispersion shifted fiber using a lattice-form programmable optical filter on a planar lightwave circuit," *J. Lightwave Technol.*, vol. 16, pp. 1647–1656, Sept. 1998.

[8] H. Tsuda, T. Kurokawa, K. Okamoto, T. Ishii, K. Naganuma, Y. Inoue, and H. Takenouchi, "Second- and third-order dispersion compensation using a high resolution arrayed-waveguide grating," in *Procl 24th Eur. Conf. Optical Commun. (ECOC'98)*, vol. 1, Madrid, Spain, Sept. 1998, pp. 533–534.

[9] H. Tsuda, K. Okamoto, T. Ishii, K. Naganuma, Y. Inoue, H. Takenouchi, and T. Kurokawa, "Second- and third-order dispersion compensator using a high resolution arrayed-waveguide grating," *IEEE Photon. Technol. Lett.*, vol. 11, pp. 569–571, May 1999.

[10] H. Tsuda, H. Takenouchi, T. Ishii, K. Okamoto, T. Goh, K. Sato, A. Hirano, T. Kurokawa, and C. Amano, "Photonic spectral encoder/decoder using an arrayed-waveguide grating for coherent optical code division multiplexing," in *Proc. Optical Fiber Commun. Conf. (OFC'99)*, vol. Postdeadline Paper PD32, Feb. 1999.

[11] ——, "Spectral encoding of 10 Gbit/s femtosecond pulses using a high resolution arrayed-waveguide grating," *Electron. Lett.*, vol. 35, no. 14, pp. 1186–1188, July 1999.
[12] ——, "Photonic spectral encoder/decoder using an arrayed-waveguide grating for coherent optical code division multiplexing," *Trends in Optics and Photonics*, vol. 29, 1999.
[13] H. Takenouchi, H. Tsuda, C. Amano, T. Goh, K. Okamoto, and T. Kurokawa, "An optical phase-shift keying direct detection receiver using a high-resolution arrayed waveguide grating," in *Proc. Optical Fiber Commun. Conf. (OFC'99)*, vol. 1, Feb. 1999, pp. 213–215.
[14] A. M. Weiner, D. E. Leaird, J. S. Patel, and J. R. Wullert II, "Programmable shaping of femtosecond optical pulses by use of 128-element liquid crystal phase modulator," *IEEE J. Quantum. Electron.*, vol. 28, pp. 908–920, Apr. 1992.
[15] C.-C. Chang, H. P. Sardesai, and A. M. Weiner, "Dispersion-free fiber transmission for femtosecond pulses by use of a dispersion-compensating fiber and a programmable pulse shaper," *Opt. Lett.*, vol. 23, no. 4, pp. 283–285, Feb. 1998.
[16] S. Shen and A. M. Weiner, "Complete dispersion compensation for 400-fs pulse transmission over 10-km fiber link using dispersion compensating fiber and spectral pulse equalizer," *IEEE Photon. Technol. Lett.*, vol. 11, pp. 827–829, July 1999.
[17] T. Goh, S. Suzuki, and A. Sugita, "Estimation of waveguide phase error in silica-based waveguides," *J. Lightwave Technol.*, vol. 15, no. 11, pp. 2107–2113, Nov. 1997.
[18] C. Dragone, "Efficient N × N star couplers using Fourier optics," *J. Lightwave Technol.*, vol. 7, pp. 479–489, Mar. 1989.

Hiroyuki Tsuda (M'99) was born in Tokyo, Japan, on February 28, 1962. He received the B.S. degree from Waseda University, Japan, in 1985, the M.E. and Ph.D. degrees from Tokyo Institute of Technology, Japan, in 1987 and 1998, respectively.

In 1987, he joined NTT Opto-electronics Laboratories, Kanagawa, Japan, where he was initially engaged in research on nonlinear optical devices including a nonlinear etalon and a bistable laser diode. In 1994, he was engaged in development of 10 Gb/s transmission systems. Since 1996, he has been researching on smart pixels with vertical cavity surface emitting lasers and on time-space conversion optical signal processing using an arrayed-waveguide grating. He is presently an Assistant Professor with the Department of Electronics and Electrical Engineering, Keio University, Japan.

Dr. Tsuda is a member of the Institute of Electronics, Information and Communication Engineers (IEICE) of Japan, the Japan Society of Applied Physics, the Optical Society of Japan, and the Optical Society of America (OSA).

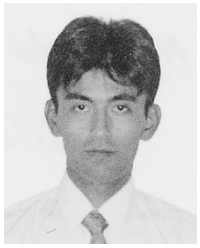

Hirokazu Takenouchi received the B.S. and M.S. degrees in pure and applied sciences from University of Tokyo, Tokyo, Japan, in 1992 and 1994, respectively.

In 1994, he joined the NTT Opto-electronics Laboratories, Kanagawa, Japan, where he was initially engaged in research on vertical-cavity surface-emitting lasers. Since 1997, he has been engaged in the research on ultrafast optical signal processing using an arrayed-waveguide grating (AWG)

Mr. Takenouchi is a member of Japan Society of Applied Physics (JSAP) and the Institute of Electronics, Information and Communication Engineers (IEICE) of Japan.

Akira Hirano was born in Hyogo Prefecture, Japan, on November 4, 1967. He received the B.S. degree in physical chemistry and M.S. degrees in astrophysics from Osaka University, Japan.

In 1993, he joined Nippon Telegraph and Telephone Corporation working in lightwave communications areas. His main interests are in the high-speed lightwave transport systems, optical signal processing and ultra short pulse generation.

Dr. Hirano is a member of The Institute of Electronics, Information and Communication Engineers (IEICE) of Japan.

Takashi Kurokawa (M'94) received the B.S. degree in pure and applied sciences, the M.S. degree in coordinate sciences, and the Ph.D. degree in basic physics from the University of Tokyo, in 1971, 1973, and 1981, respectively.

In 1973, he joined NTT Laboratories, where he was initially engaged in pioneering work on organic optical waveguides. From 1988 to 1998, he was engaged in studies of optical processing and switching, and their devices as a Leader of Optical Signal Processing Device Research Group at NTT Opto-electronics Laboratories, Kanagawa, Japan. Since April 1998, he has been a Professor of Electrical and Electronic Engineering at Tokyo University of Agriculture and Technology, Tokyo. He has published more than 150 papers, book chapters, and articles on his research interests, which currently include optical signal processing, optical interconnects, optoelectronic device design, and image sensing.

Dr.Kurokawa has served on committees for the Japan Society of Applied Physics, for the Institute of Electronics, Information and Communication Engineers (IEICE) of Japan, for the Optical Society of Japan, for the IEEE Lasers and Electro-Optics Society (LEOS), for the Optical Society of America (OSA), for Optoelectronic Industry and Technology Development Association, and on some scientific editorial boards.

Katsunari Okamoto (M'85–SM'98) was born in Hiroshima, Japan, on October 19, 1949. He received the B.S., M.S., and Ph.D. degrees in electronics engineering from Tokyo University, Tokyo, Japan, in 1972, 1974, and 1977, respectively.

He joined Ibaraki Electrical Communication Laboratory, Nippon Telegraph and Telephone Corporation, Ibaraki, Japan, in 1977, and was engaged in the research on transmission characteristics of multimode, dispersion-flattened single-mode, single-polarization (PANDA) fibers, and fiber-optic components. As for the dispersion-flattened fibers (DSF), he first proposed the idea and confirmed experimentally. From September 1982 to September 1983, he joined Optical Fiber Group, Southhampton University, Southampton, U.K., where he was engaged in the research on birefringent (Bow-tie) optical fibers. Since October 1988, he has been working on the analysis and synthesis of the guided-wave devices, the computer-aided design (CAD), and fabrication of the silica-based planar lightwave circuits at Ibaraki R&D Center, NTT Opto-electronics Laboratories. He has developed 128ch-25 GHz spacing AWGs, flat spectral response AWGs and integrated-optic add–drop multiplexers. He is presently a research fellow at the Okamoto Research Laboratory in NTT Photonics Laboratories. He has served as a LEOS Distinguished Lecturer (1997–1998). He published more than 100 papers and authored or coauthored eight books.

Dr. Okamoto is a member of the Optical Society of America (OSA), the Institute of Electroncis, Information and Communication Engineers (IEICE) of Japan and the Japan Society of Applied Physics.